Astron. Astrophys. 267, 586–594 (1993)

ASTRONOMY AND ASTROPHYSICS

Dynamics of flaring loops

III. Interpretation of flare evolution in the emission measure–temperature diagram

B. Sylwester[1], J. Sylwester[1], S. Serio[2,3], F. Reale[2], R.D. Bentley[4], and A. Fludra[4]

[1] Space Research Centre, Polish Academy of Sciences, ul. Kopernika 11, PL-51-622 Wrocław, Poland
[2] Istituto di Astronomia and Osservatorio Astronomico, I-90134, Palermo, Italy
[3] Istituto per le Applicazioni Interdisciplinari della Fisica, CNR, I-90134 Palermo, Italy
[4] Mullard Space Science Laboratory, Holmbury St. Mary, Dorking, Surrey, GB-RH5 6NT, United Kingdom

Received May 4, accepted June 1, 1992

Abstract. The aim of the paper is to illustrate the application of the density–temperature diagrams discussed in the previous paper (Paper II) to interpretation of soft X-ray measurements namely calcium spectra recorded by the Solar Maximum Mission *Bent Crystal Spectrometer*. First, using the emission measure (ε_{Ca}) and the temperature (T_{Ca}) values derived for a set of hydrodynamic (HD) flare models discussed in previous papers, we have obtained and analysed the ($\sqrt{\varepsilon}$–T) counterparts of the (N–T) diagrams. Inspection of these diagrams reveals that they qualitatively resemble the (N–T) diagrams. The inclinations of the decay trajectories make the main difference. Next, we have performed a comparison of the modelled and observed flare evolutionary trajectories. This comparison allowed us to identify characteristic cases of evolution during the decay phase. We have discussed time variations of the heating rate for selected observed flares. The results of this paper illustrate how to use the diagnostic diagrams in the interpretation of flare soft X-ray measurements.

Key words: Sun – flares – heating rate diagnostics

1. Introduction

In the previous paper of this series (see Jakimiec et al. 1992; hereafter Paper II) the theoretical bases of the flare heating diagnostic method have been presented. A number of simple models of a single flaring loop of constant cross sectional area calculated by means of the Palermo–Harvard hydrodynamic code (Peres et al. 1982) have been considered. The evolution of basic thermodynamic parameters of a flaring plasma has been analyzed in the density–temperature (N–T) diagrams. It turned out that the (N–T) diagrams constitute diagnostic diagrams for the heating function $E_H(t)$, which is an important physical quantity. Investigations of the heating function are of great significance since it describes the rate of thermal energy release in solar flares i.e. the flare heating process.

The main conclusions of Paper II are as follows:

(a) Specific changes of the heating function $E_H(t)$ cause related characteristic evolutionary patterns in the (N–T) diagram.

(b) During the heating phase, the plasma temperature at the loop top adjusts quickly ($t < 20$ s) to the actual value of energy deposition rate through direct conductive coupling of the heated plasma with cooler regions; its value is close to that corresponding to the steady-state conditions.

(c) During the cooling phase, two characteristic limiting branches of the flare evolution can be distinguished in the (N–T) diagrams:

— a branch of fast cooling when the flare heating decreases quickly enough (the slope of this branch is $d(\log T_{top})/d(\log N_{top}) = \xi \approx 2.0$)

— a so-called quasi-steady-state (QSS) branch ($\xi \approx 0.5$) when the heating function decreases is sufficiently slow.

In the present paper, we shall discuss how to take advantage of the conclusions of Paper II in the interpretation of solar flare soft X-ray observations. In particular we shall concentrate on the analysis of the calcium spectra obtained by means of the *Bent Crystal Spectrometer* (*BCS*) on the Solar Maximum Mission satellite. We have chosen the Ca spectra since their time resolution is sufficiently high for our purposes and the emission in Ca lines is strong enough relatively early during the flare rise phase.

Acton et al. (1980) gave a detailed description of the *BCS* spectrometer; the method of data reduction and fitting procedure has been given by Fludra et al. (1989) and references therein.

In Sect. 2 we discuss the comparison between the theoretical and empirical flaring plasma parameters and express the (N–T) diagnostic diagrams for the models presented in Paper II in terms of observables, i.e. the temperature T_{Ca} and the emission measure ε_{Ca}. A short description of the data and a comparison of calculated and actually observed flare evolution in emission measure–temperature diagrams for a sample of the BCS data is presented in Sect. 3. Section 4 is devoted to a summary and conclusions.

2. Flare evolution in the emission measure–temperature diagram

In the earlier papers (Jakimiec et al. 1986, 1987) the method of analysis of the flare evolution (presented in detail in Paper II) has been introduced. Observational counterparts of the theoretical (N–T) diagrams have been illustrated there. Such observational counterparts are very important qualitatively but they are built on flare characteristics different from the summit temperature and density used in the (N–T) diagrams. Therefore in this section,

Send offprint requests to: B. Sylwester

we transpose the (N–T) diagrams for models considered in Paper II into diagrams which allow for a direct comparison with observations. The summit temperature and density in the diagrams are represented now by the temperature T_{Ca} and emission measure ε_{Ca}, respectively. These quantities are obtained from the isothermal interpretation of calcium spectra ($\lambda \approx 3.2$ Å) recorded by the BCS instrument on SMM.

The intensity F_i of an X-ray spectral line i emitted by an optically thin coronal plasma is expressed as

$$F_i = \int f_i(T)\, \varphi(T)\, \mathrm{d}T, \tag{1}$$

where $f_i(T)$ is the emission function (i.e. the temperature-dependent line intensity for unit emission measure of the plasma, as predicted by the theory for assumed elemental abundance) and $\varphi(T) = N_e^2\, \mathrm{d}V/\mathrm{d}T$ is the differential emission measure distribution. The isothermal approximation is often used in the analysis of soft X-ray spectra. It is known (see Jakimiec et al. 1987) that the isothermal approach is generally an oversimplification. According to present solar flare models, the flaring plasma is confined in coronal magnetic structures and is distributed with temperature. The main shortcomings of the isothermal approximation have been discussed by Jakimiec et al. (1987). However, this simple approximation is convenient in the interpretation of the fluxes for lines characterized by slightly different emission functions (Sylwester 1990).

The temperature T_{ij} in the isothermal approximation is derived from the ratio of fluxes in spectral lines i and j with emission functions $f_i(T)$ and $f_j(T)$. For a given pair of line fluxes (F_i and F_j) a corresponding pair of temperature and emission measure (T_{ij}, ε_{ij}) can be attributed.

In order to determine the quantitative relation between T_{Ca} and T_{top} in the case of simple flare models, fluxes in k and w lines of Ca ions (F_w, F_k) have been calculated according to Eq. (1), incorporating the same emission functions as in the paper of Fludra et al. (1989). The temperature T_{Ca} has been calculated based on the F_w/F_k ratio for all moments throughout the calculated evolution of flares. Derived temperatures (T_{Ca}) have been compared with temperatures of the plasma at the top of the loop (T_{top}).

In Fig. 1 we present results of the comparison of T_{Ca} and T_{top} for 32 different models (see Table 1 of Paper II). We have taken into account only those time intervals of evolution for which the Ca spectra are strong enough ($t > 40$ s from the start of the flare heating). It is seen from the figure that a clear relationship exists between the temperature T_{Ca} and T_{top} for the sample of flare models. One can regard T_{Ca} a good characteristic of T_{top}. It should be noticed that T_{Ca} is always lower than T_{top} (the difference being the smallest for lower temperatures), since T_{Ca} is the average temperature over the (relatively big) flare volume where Ca lines are effectively formed ($T > 6.5$ MK).

A similar simple relation exists between ε_{Ca} as derived from the intensity of the resonance line w and the actual total emission measure of the soft X-ray flare volume. Since in flare models this volume is approximately constant during the flare development, $\sqrt{\varepsilon_{Ca}}$ is a characteristic of N_{top}:

$$\varepsilon_{Ca} \approx N_{top}^2\, V. \tag{2}$$

Values of the parameters T_{Ca} and ε_{Ca} have been used to draw diagnostic diagrams T_{Ca} vs. $\sqrt{\varepsilon_{Ca}}$ for each flare model. In the following analysis we shall refer to these diagrams as ($\sqrt{\varepsilon}$–T) for brevity. An example of such a diagram is shown in Fig. 2, where the pattern of evolution for the family of decay phase models (SS–OFF) considered in Papers I and II is presented. The notation for individual models is according to Table 1 of Paper I. Original (N–T) diagrams for these models have been presented in Fig. 2 of Paper II. As in the case of the (N–T) diagrams the SS-OFF models demonstrate a characteristic pattern of the evolution. The average slope of all evolutionary trajectories during a relatively long period of the decay is similar, nearly independent of the loop semilength or the initial temperature. The average slope for all SS–OFF models presented in Fig. 2 is $\zeta = \mathrm{d}(\log T_{Ca})/\mathrm{d}(\log \sqrt{\varepsilon_{Ca}}) = 1.46 \pm 0.14$.

The corresponding slope in the (N–T) diagram was substantially greater ($\xi = 1.96 \pm 0.17$, cf. Paper II).

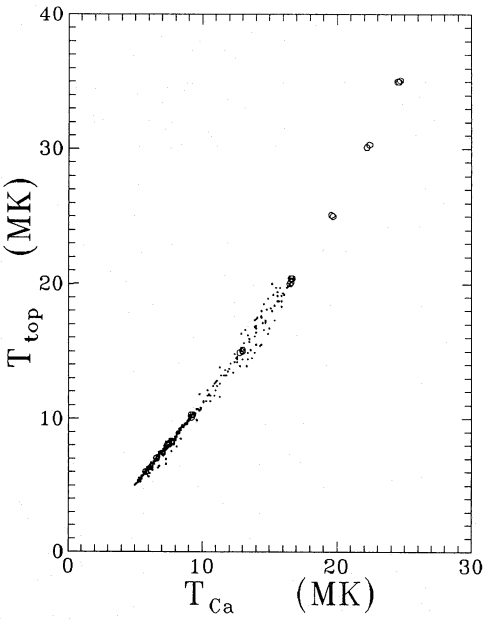

Fig. 1. A comparison of summit temperature (T_{top}) as taken from hydrodynamic flare models with the temperature (T_{Ca}) obtained for a given model from the k and w line intensity ratio (isothermal approximation, see text for details). The open circles are related to steady-state models

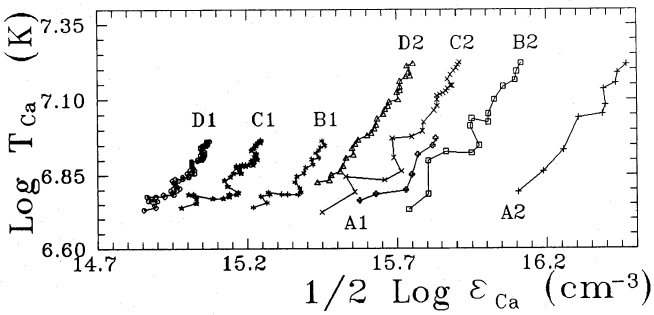

Fig. 2. The emission measure–temperature (ε–T) diagram for decay phase models (SS-OFF). The letters A, B, C and D in the figure correspond to semilengths of 5, 20, 50 and 100 Mm, respectively, and the numbers 1 and 2 represent the initial maximum temperature in units of 10 MK. (This notation is according to previous papers of this series.)

Similarly, for other models analysed in Paper II, all characteristic phases of the flare evolution which have been distinguished in the (N–T) diagrams are present in the ($\sqrt{\varepsilon}$–T) diagrams too. However, for the models with the heating kept constant during the initial phase, the evolutionary trajectories during the **b**-phase do not run exactly horizontally as in the case of the (N–T) diagrams. This could be related to a complicated temperature structure of the plasma during early flare phases. But under a sufficiently long-lasting constant heating, the temperature T_{Ca} stabilizes and the evolutionary paths run nearly horizontally.

The pattern for the cooling phases resembles that in the (N–T) diagrams, although, as in the case of SS–OFF models, an important difference could be noticed between the average slopes during the **d**-phase.

The straight line which represented a steady-state (S-S) relation between plotted parameters had the slope $\zeta_{S\text{-}S}=0.5$ in the (N–T) diagrams. Now, when expressed in terms of $\sqrt{\varepsilon_{Ca}}$ and T_{Ca} this slope is $\zeta_{S\text{-}S}=0.37\pm0.01$. Inspection of the ($\sqrt{\varepsilon}$–$T$) diagrams shows that most of the conclusions concerning the flare evolution in the (N–T) diagrams remain valid. This allows for the diagnostics of flare energy release rate, $E_H(t)$, based on the interpretation of BCS line spectra.

In particular, for the cooling phases, two characteristic limiting branches of flare evolution have now the following slopes in the ($\sqrt{\varepsilon}$–T) diagrams:

(1) $\zeta\approx1.46$ for the branch of fast cooling, when the flare heating decreases quickly ($\tau\leq60$ s for the case of $L=20$ Mm),

(2) $\zeta\approx0.37$ for the QSS-branch of evolution, when the heating function decrease is sufficiently slow ($\tau\geq1200$ s for $L=20$ Mm).

To investigate the functional dependence $\zeta(\tau)$ for intermediate values of τ we have extended the set of considered hydrodynamic model calculations. We have carried out the calculations for models initially in steady-state conditions ($L=20$ Mm, initial value of $T_{top}=20$ MK), with several e-folding decay times of the heating rate ($\tau=60, 180, 300, 1200$ s). For the case of $\tau=300$ s additional calculations have been performed for two other, significantly different loop semilengths ($L=50$ and 100 Mm) and for two initial values of the top temperature ($T_{top}=10$ and 20 MK). The results of the analysis of the ($\sqrt{\varepsilon}$–T) diagrams for this set indicate, that, in contrast to the OFF and QSS branches, the inclination of the evolutionary trajectory depends on the loop semilength L. We have noticed that this dependence cancels out if the decay time τ of the heating rate is expressed in units of the entropy decay time τ_{th} [Eq. (14) in Paper I]. In Fig. 3 we present a combined plot of the inclination ζ vs. τ/τ_{th} where the included points correspond to $\tau\neq0$ cases for which the initial conditions are steady-state ones, also those with different loop semilengths L. The slopes corresponding to the limiting branches (QSS and OFF) are indicated. They are asymptotically reached when τ/τ_{th} is large ($\tau/\tau_{th}>6$) or small ($\tau/\tau_{th}<0.2$), respectively.

As discussed in Paper II, when the evolution proceeds along the QSS-branch then the actual rate of energy release into the flare volume is related to other loop parameters according to:

$$E_H \cong 1.0\,10^{-6}\,T_{top}^{3.5}\,L^{-2}. \quad (3)$$

This formula is valid also during most of the flare rise phase, as was noticed by Jakimiec et al. (1986). For the calculated loop models (during the rise phase) the relation (3) is valid to within a 20% accuracy for various heating rates, time profiles of the heating and loop semilengths (Sylwester 1988).

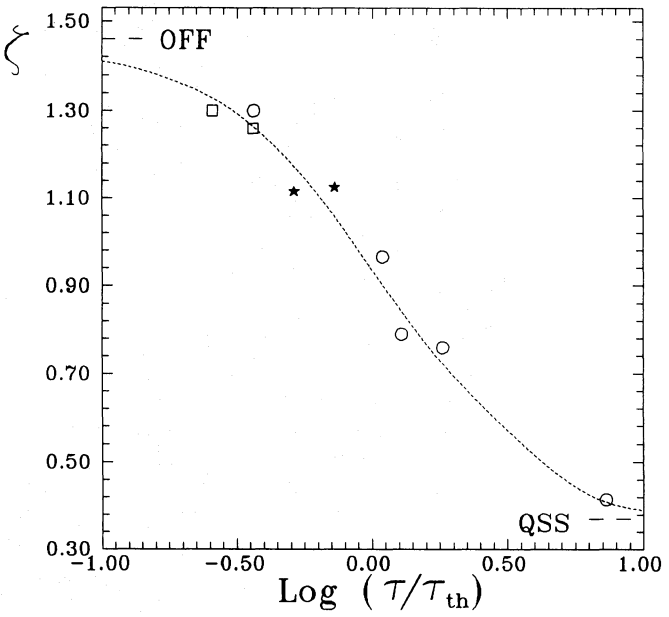

Fig. 3. The dependence of the slope ζ on the e-folding decay time of the heating (τ) expressed in units of the thermodynamic decay time (τ_{th}) (cf. Paper I). The points plotted correspond to models starting from steady-state conditions ($T_{top}=20$ MK) for loops of various semilengths: 20 (°), 50 (*) and 100 Mm (□)

So, for those observed flares for which estimations of the flare lengths are possible, the absolute value of the heating rate can be estimated based on Eq. (3) and the T_{Ca}–T_{top} relationship (cf. Fig. 1). If the heating rate during the flare growth phase is not constant in time, one can estimate its logarithmic increment/decrement based on this relation – the knowledge of L is not necessary for this purpose.

When the flare evolves along the QSS-branch, we can estimate the characteristic time τ of the heating rate decrease, from the observed decay time of the temperature $d(\log T_{Ca})/dt$.

From the above discussion it follows that the analysis of the emission measure–temperature diagrams is very helpful in a determination of the qualitative and quantitative changes of heating rate throughout the flare evolution. In the following section, we shall present such an analysis for selected flares.

3. Data description and the analysis

Our data consist of the X-ray spectra of highly-ionized calcium ($\lambda\cong3.17$–3.24 Å) which have been measured by the BCS on board the SMM satellite. The entire synthetic spectrum of Ca XVIII–XIX lines has been fitted to the measured one using a two-component (stationary and moving) fitting procedure (Fludra et al. 1989). In the process of fitting, the temperatures T_{Ca} of the two components have been assumed to be equal and have been derived from the k/w line intensity ratio for the stationary component. Here, we are not interested in the analysis of plasma motions since they do not directly influence the results of our study. Therefore we have used the sum ε_{Ca} of the emission measures for the stationary and blueshifted (moving) component as a characteristic of the entire emitting volume. The sequence of

T_{Ca} and ε_{Ca} values has been determined from fits to all available spectra (20 s accumulation time) for a given flare. In order to avoid a scatter due to statistics, we usually have made consecutive averaging over 5 points (about 1.5 min) before constructing the emission measure–temperature diagram. As a rule, during the rise phase few spectra were available only, so non-averaged data have been used during that time. For short duration flares the non-averaged data have been used throughout the flare.

We have analysed a total of 66 solar flares observed by the BCS during 1980–1987. The list of flares containing selected flare characteristics is given in Table 1. For eight of them the ($\sqrt{\varepsilon}$–T) diagrams have been presented in previous papers (Jakimiec et al. 1986, 1987; Sylwester 1988; Sylwester et al. 1990a, b). In those earlier interpretations we did not take into account the T_{Ca}–T_{top} rescaling. The inspection of the ($\sqrt{\varepsilon}$–T) diagrams for flares analysed in this paper showed that five groups can be distinguished with regard to the character of the evolutionary path during the decay:

(I) OFF-like which have slopes of the decay phase close to those obtained for models with an abrupt switch-off or with fast decay of the heating ($\tau/\tau_{th}<0.2$), cf. Fig. 4;

(II) QSS-like, with slopes corresponding to models with quasi-steady-state evolution (very slow heating rate decay, $\tau/\tau_{th}>5$), cf. Fig. 5a, b;

(III) intermediate, having slopes between those for OFF- and QSS-like cases, cf. Fig. 6a–c;

(IV) those characterized by decay phase slopes not predicted by the considered simple flare models (i.e. steeper than the OFF-like branch slope or flatter than the QSS-like slope), cf. Fig. 7;

(V) those for which the decay phase of the evolutionary path is composed of two or more branches having different inclinations, cf. Fig. 8a, b.

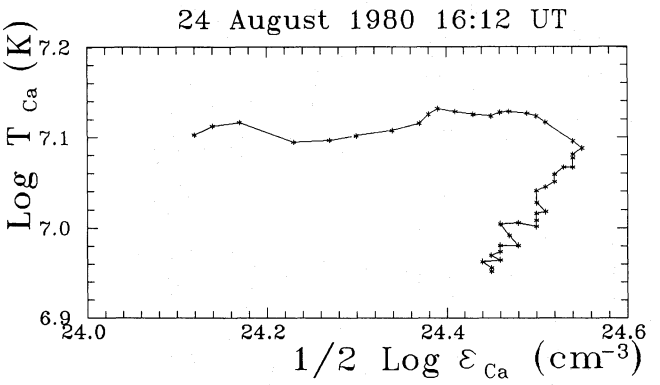

Fig. 4. The emission measure–temperature diagram for the flare on 24 August 1980 at 16:12 UT

In Fig. 4 the ($\sqrt{\varepsilon}$–T) diagram for the flare on 24 August 1980 at 16:12 UT (BCS maximum) is shown. This flare, according to Hα and GOES classification was SB and M 1.0, respectively. The flare lasted for about 25 min in soft X-rays. The observed pattern of evolution suggests that this flare belongs to group I, the OFF-like. During the heating period, lasting at least for 360 s, the rate of heating appears to be nearly constant. The following evolution suggests that the heating has been decreasing with a very short characteristic decay time $\tau/\tau_{th}\approx 0.2$ (the evolutionary pattern during the decay phase has the inclination $\zeta=1.32$). Regular pattern of decay evolution lasted for about 500 s.

Two examples of ($\sqrt{\varepsilon}$–T) diagrams representative of the II group (the QSS-like) are presented in Fig. 5a, b. The flare shown in Fig. 5a (7th April 1980 at 05:40 UT; 1B, M 8.0) lasted for about 20 min. It was a gradual rise and fall event. The size of main kernel of the flare as observed by the HXIS instrument aboard the SMM was estimated as $2L=20$ Mm (Machado et al. 1983). As in the previous case, nearly constant heating during the rise phase is observed ($E_H=25$ erg cm^{-3} s^{-1}). For about 11 min of the early decay phase a quasi-steady-state evolution took place. As discussed earlier, for the QSS-like evolution we can estimate τ based on the decay time of the temperature; we have obtained $\tau\approx 630$ s.

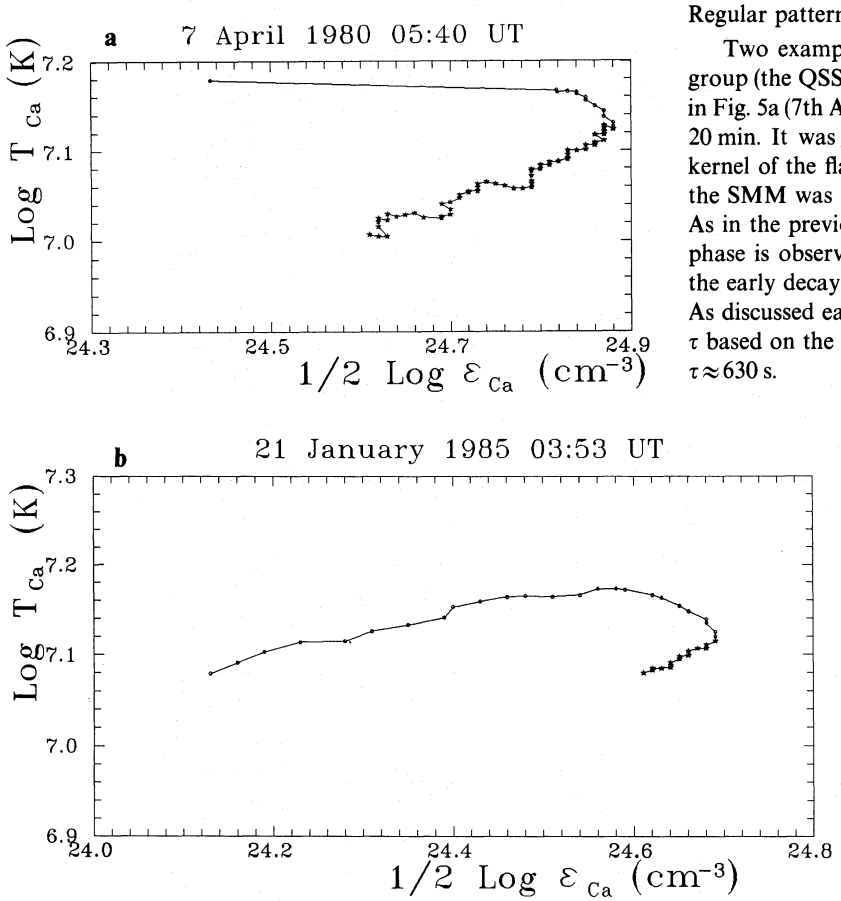

Fig. 5a and b. The emission measure–temperature diagrams for the flares on 1980 April 7 at 05:40 UT (**a**) and on 1985 Jan. 21 at 03:53 UT (**b**)

Table 1. List of studied flares

No.	Data	Time[a] (UT)	Active region	Coordinates	GOES class	Duration[b] (s)	Group[c]	Comments
1	1980 Apr 07	01:09	2372	N10 E03	M4.0	2000	V	
2	1980 Apr. 07	05:40	2372	N12 E01	M8.0	1800	II	
3	1980 Apr. 08	03:07	2372	N12 W13	M4.0	1525	III	
4	1980 Apr. 10	09:22	2372	N12 W42	M4.0	720	V	
5	1980 Apr. 13	04:08	2372	N10 W77	M1.0	990	IV	
6	1980 Apr. 30	20:25	2396	S13 W90	M2.2	310	II	L
7	1980 May 07	14:57	2418	S22 W12	C7.0	150	II	
8	1980 May 09	07:14	2418	S21 W32	M7.0	635	V	
9	1980 May 21	21:05	2456	S14 W15	X1.4	665	V	
10	1980 June 04	09:12	2490	S13 E58	M4.0	2539	II	D
11	1980 June 21	01:02	2528	S12 E17	M2.0	1523	V	
12	1980 June 24	15:24	2522	S29 W15	M1.0	280	IV	
13	1980 June 29	02:38	2522	S27 W90	M3.6	1440	III	L
14	1980 June 29	10:43	2522	S24 W90	M4.2	1110	III	L
15	1980 June 29	18:26	2522	S20 W90	M4.2	825	III	L
16	1980 July 01	16:28	2544	S12 W38	X2.5	831	V	
17	1980 July 05	22:45	2550	N28 W31	M8.9	3195	V	
18	1980 July 11	22:18	2562	S10 E70	M5.3	360	V	D
19	1980 July 12	11:19	2562	S14 E56	M4.3	983	IV	
20	1980 July 14	08:27	2562	S13 E43	X1.1	440	II	
21	1980 July 17	06:11	2562	S12 E06	M3.4	380	IV	D
22	1980 July 21	03:00	2562	S14 W60	M8.0	612	V	
23	1980 Aug. 23	21:30	2629	N16 W39	M2.1	480	I	
24	1980 Aug. 24	16:12	2629	N17 W52	M1.0	1065	I	
25	1980 Aug. 25	13:05	2629	N18 W62	M1.0	840	I	
26	1980 Aug. 31	12:49	2646	N12 E28		120	I	
27	1980 Aug. 31	12:52	2646	N12 E28	M2.8	170	II	
28	1980 Oct. 14	05:45	2725	S09 W07	M1.8	515	I	
29	1980 Oct. 14	06:14	2725	S09 W07	X3.3	2110	V	
30	1980 Oct. 20	18:34	2744	S17 E45	M1.0	245	II	
31	1980 Nov. 05	22:29	2776	N11 E07		230	III	
32	1980 Nov. 05	22:35	2776	N11 E07	M4.0	350	I	
33	1980 Nov. 06	17:28	2779	S09 E65	M4.2	1570	I	
34	1980 Nov. 07	04:58	2779	S10 E57	M2.5	1745	II	
35	1980 Nov. 07	09:40	2779	S06 E59	M1.2		I	D
36	1980 Nov. 12	02:52	2779	S13 W06	M1.9	965	I	
37	1980 Nov. 12	11:07	2779	S12 W10	C8.6	195	IV	
38	1980 Nov. 12	17:05	2779	S14 W11	M1.4	390	IV	
39	1980 Nov. 12	17:37	2779	S13 W15	C7.0	372	IV	
40	1980 Nov. 13	00:50	2779	S11 W21	M9.4	1750	V	D
41	1980 Nov. 18	14:55	2779	S10 W90	M3.0	590	II	L
42	1980 Nov. 19	05:45	2779	S10 W90	M6.0	1008	V	L
43	1980 Nov. 22	05:38	2793	N12 W02	C9.0	341	III	
44	1984 Apr. 26	09:03	4474	S09 E34	M2.5	698	II	
45	1984 Apr. 27	05:41	4474	S10 E24	M2.3	334	I	
46	1984 Apr. 30	05:56	4474	S14 W34	M1.1	94	IV	
47	1984 Apr. 30	11:55	4474	S12 W31	M2.3		III	D
48	1984 May 01	01:34	4474	S14 W32	M4.0		V	
49	1984 May 02	19:26	4474	S11 W58	M3.0	2034	IV	
50	1984 May 03	03:18	4474	S12 W67	C7.1	715	I	
51	1984 May 19	21:56	4492	S10 E66	X4.1	1720	V	
52	1984 May 20	01:14	4492	S10 E64	C4.5	58	I	
53	1984 May 20	01:29	4492	S10 E64	M2.9	628	III	
54	1984 May 20	02:53	4492	S13 E62	C7.0	268	IV	
55	1984 May 20	03:01	4492	S13 E62	M4.6	1189	V	
56	1984 May 20	05:43	4492	S08 E57	M5.4	540	V	

Table 1 (continued)

No.	Date	Time[a] (UT)	Active region	Coordinates	GOES class	Duration[b] (s)	Group[c]	Comments
57	1984 May 20	06:21	4492	S08 E57	M1.0	276	II	
58	1984 May 20	22:39	4492	S08 E52	X10		III	D
59	1984 May 21	17:47	4492	S06 E42	C7.0	258	IV	
60	1984 May 21	18:10	4492	S08 E42	X3.0	1365	III	
61	1985 Jan. 20	20:51	4617	S09 W24	M4.1	1509	V	
62	1985 Jan. 21	03:53	4617	S10 W28	M2.2	1003	II	
63	1985 Apr. 24	01:52	4647	N03 E27	C8.8	829	IV	
64	1985 May 02	07:40	4647	N03 W86	M4.0		II	D
65	1985 July 02	21:26	4671	S15 E56	M4.5	1868	II	
66	1987 Apr. 06	04:33	4787	S28 E86	C9.2	412	III	

Notes to Table 1: D: Decay phase recorded only.
L: Limb flare.
The data on NOAA active regions and GOES classification have been taken from Solar Geophysical Data and from Speich et al. (1991).
[a] The time of maximum flux observed in the BCS Ca channel. When the Ca spectra have been recorded during the decay phase only, then the time indicated denotes the time of maximum flux in soft X-ray GOES data.
[b] Duration of the event in seconds as recorded by the HXRBS on SMM. These data have been taken from Dennis et al. (1988).
[c] The numbers I–V denote the character of flare evolution according to one of five generic evolutionary patterns in the emission measure–temperature diagrams. See text for the details.

The flare shown in Fig. 5b (21st January 1985 at 03:53 UT; 1B, M 2.2) was also a long-lasting one. Only part of the decay phase was recorded by the BCS (about 5 min), but unambiguously during this period the evolution proceeds along the QSS-branch. The e-folding decay time of the heating rate is $\tau \cong 1300$ s in this case. During the rise phase of this flare an increase of heating rate is observed with e-folding time of 300 s.

Three examples of diagrams corresponding to the group III are presented in Fig. 6a–c. The flare presented in Fig. 6a (22 Nov. 1980 at 05:08 UT; 2N, C 9.0) has been examined previously by Chung-Chieh Cheng & Pallavicini (1984) and by Sylwester et al. (1986). This flare was a gradual rise and fall event, relatively long-lasting in soft X-rays (about 40 min). It is related to a large soft X-ray loop-like structure located near the central meridian. According to *FCS* observations the loop was of $L \approx 50$ Mm semi-length. During the decay, the observed inclination ($\zeta = 0.65$) of the evolutionary path is in agreement with the heating rate e-folding decay time of $\tau \approx 1100$ s. The absolute value of the maximum heating rate for this flare, cf. Eq. (3), was moderate ($E_H \approx 1$ erg cm^{-3} s^{-1}). It should be noticed that this value is about twice as high as that obtained in the paper by Sylwester et al. (1986) for the same flare (in the previous paper we did not rescale the observed temperature T_{Ca} to T_{top}).

The flare presented in Fig. 6b (20 May 1984 at 01:29 UT; 1B, M 2.9), characterized by a steep rise (during 5 min) and gradual fall (during 10 min) has been observed from the onset. During the rise phase the heating rate increases at least 10 times and later on it was constant for a short period. For about 600 s during the decay phase, the observed inclination was $\zeta = 0.55$. For this flare an estimation of the loop semilength is not available. If we assume the loop semilength to be 20 Mm or 100 Mm then the e-folding decay time would be $\tau \approx 650$ or 3300 s, respectively.

The evolution of a flare of 6th April 1987 (04:33 UT; SN, C9.2) is presented in Fig. 6c. The flare duration was about 10 min. In case of this flare the heating rate systematically decreases during the observed part of the rise phase with an e-folding time of 85 s. The slope $\zeta = 0.95$ is observed during 180 s of the decay phase. As in the previous case, for $L = 20$ or 100 Mm, the appropriate values of τ would be 200 or 1000 s, respectively.

Examples of group IV flares are presented in Fig. 7. Both flares (12th November 1980 at 17:05 UT; 1B, M1.4 and at 17:37 UT; SN, C7.0) were related to the same active region and each lasted for about 20 min. The heating rates apparently have not been constant during the rise phases: their respective E_H values increased nearly twofold during 115 s of the rise for the stronger flare, and during 460 s for the fainter one. For both flares the inclination during the decay is steeper than the OFF-like limit. These flares probably correspond to loop structures for which the ratio of length/cross sectional area is decreasing during the decay and/or to those which are nonuniformly heated across the loop (Sylwester et al. 1990 a, b).

An example of the ($\sqrt{\varepsilon}$–T) diagrams for two flares of group V is presented in Fig. 8a, b. The first flare (10th April 1980 at 09:22 UT; 1N, M 4.0) has been observed by the BCS for about 20 min. The interpretation of HXIS images of this flare (Duijveman et al. 1982; Duijveman & Hoyng 1983) indicates that the harder and softer X-ray sources were different in shape. The harder image (10-22-30 keV) was made up of two bright patches while the softer X-ray emission (3.5–5.5 keV) was formed in between the harder patches. The loop semilength derived from HXIS images is 20 or 12 Mm depending on whether the soft or hard source is considered. These lengths allow us to estimate the corresponding heating rates as $E_H = 6$ or 17 erg cm^{-3} s^{-1}. The heating operated at a constant level for about 240 s during the

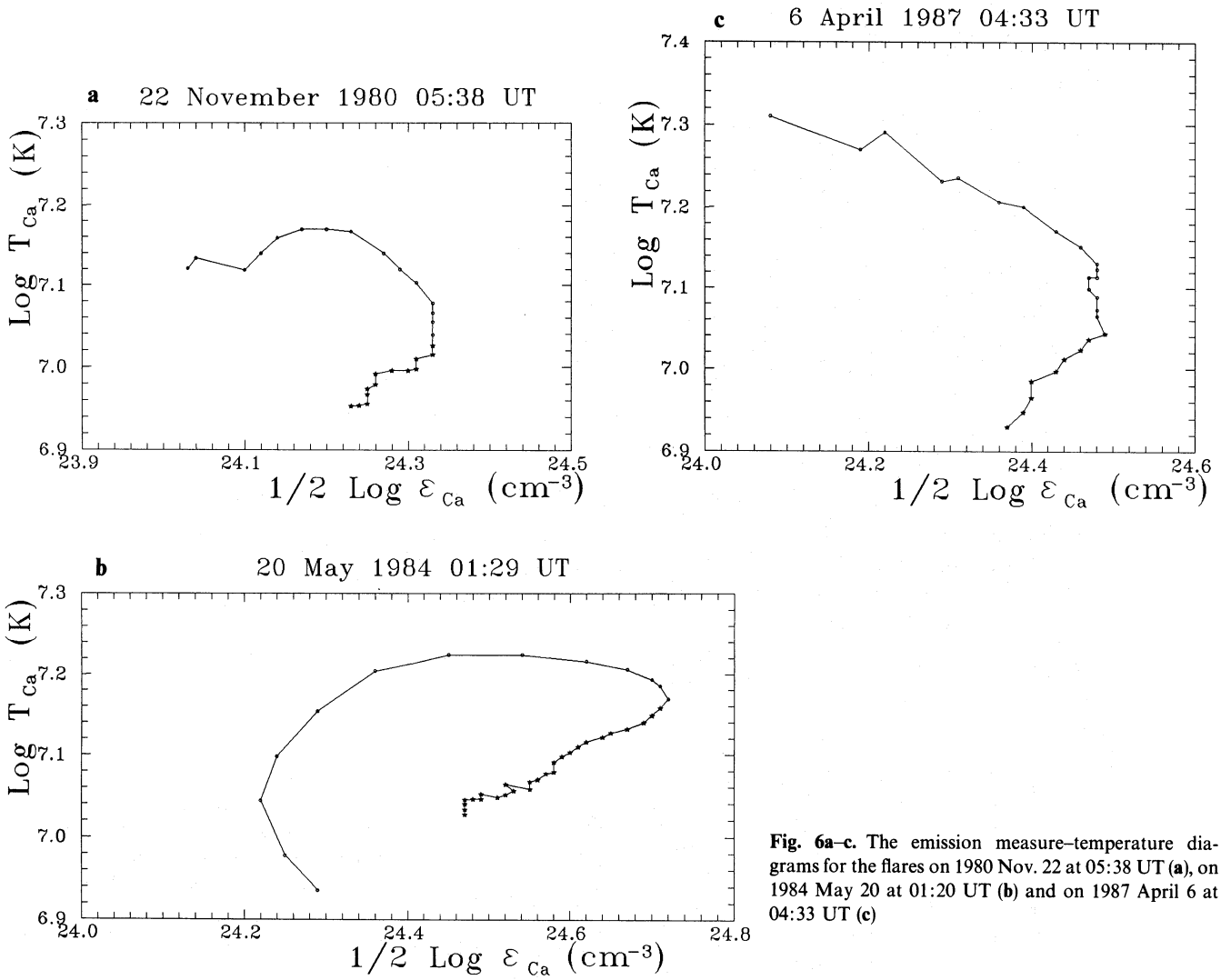

Fig. 6a–c. The emission measure–temperature diagrams for the flares on 1980 Nov. 22 at 05:38 UT (**a**), on 1984 May 20 at 01:20 UT (**b**) and on 1987 April 6 at 04:33 UT (**c**)

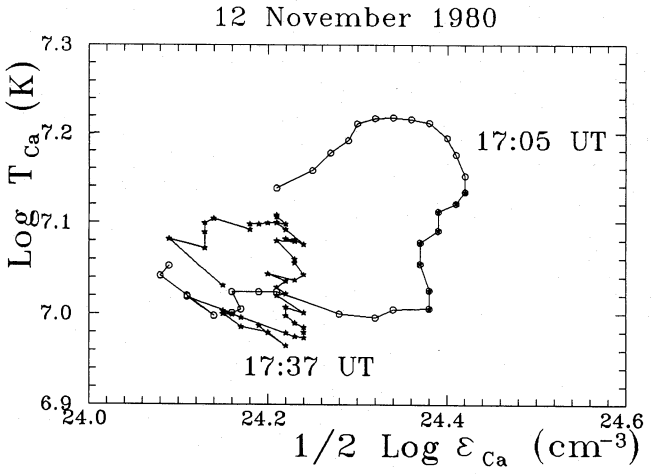

Fig. 7. The emission measure–temperature diagrams for two flares on 1980 Nov. 12 at 17:05 UT and 17:37 UT

rise phase. During the decay, two evolutionary branches can be distinguished. Corresponding slopes ($\zeta_1 = 1.7$ and $\zeta_2 = 0.3$) are beyond the limits defined by the OFF- and the QSS-like cases.

In Fig. 8b the evolution of the 9 May 1980 flare (07:14 UT; 1B, M 7) is presented. An extensive analysis of HXIS images of this flare and their comparison with Hα spectroheliograms has been performed by Machado (1983). He has found that throughout the duration of the event more than 90% of the X-ray emission came from a small region (a small loop or loop system) of size comparable to that of the Hα flare. Based on the combination of X-ray and Hα data he has estimated the loop length ($2L$) as 15 Mm. He has concluded his analysis of the energy balance in this flare saying that "... *the energy input requirements are such that* $\sim 10^2$ *erg cm*$^{-3}$ *s*$^{-1}$ *have to be released within the flare structure(s)*...".

Other studies of the same event have been performed based on the analysis of high-resolution soft X-ray spectra recorded by the NRL experiment *SOLFLEX* (Doschek et al. 1981). They estimated the peak density of about 10^{12} cm^{-3} at 07:13 UT and of about $3.5\,10^{11}$ cm^{-3} at 07:22 UT from the forbidden to intercombination line ratio in O VII ($T \approx 2$ MK).

From Fig. 8b it is seen that during 100 s of the rise phase the heating rate is approximately constant [$E_H \approx 90$ erg cm^{-3} s^{-1}, as derived from Eq. (3)], which is in close agreement with the estimate obtained by Machado (1983). During 240 s of the early decay phase the inclination of the evolutionary pattern is $\zeta = 0.75$,

which leads to a heating rate decay time $\tau \approx 520$ s. Later on (after 07:19 UT) a QSS-like branch of the evolution is observed for more than 400 s. During this period $\tau \approx 130$ s as derived from dT/dt. The two-branch decay pattern in Fig. 8b seems to indicate that the emission arises in two physically distinct loop structures which successively dominate the soft X-ray radiation during the decay. The loop dominating earlier has a rather short thermodynamic decay time and decay time of heating and therefore cools quickly. After 07:19 UT this loop is on the decline and the intensity of the Ca lines is dominated by the radiation from the other loop. This other loop evolves along the QSS branch.

Most of the 66 analyzed flares show a simple behaviour in the $(\sqrt{\varepsilon}-T)$ diagram (group I consists of 12 events, II of 14, III of 11 and IV of 12). Numerous flares belong to group V (17 cases). The observed distribution of flares among different groups is representative mainly for bigger flares (the selection of stronger flares by the BCS instrument). Big flares are usually more complicated, with different individual structures contributing at the same time to soft X-rays. This may explain why all of the strongest flares (GOES X importance) belong to group V characterized by a rather complicated behaviour in the $(\sqrt{\varepsilon}-T)$ diagram. For flares of group I–III, conditions close to those assumed in the hydrodynmic modelling are more appropriate with respect to the flare geometry and heating rate. For flares from group IV the approximation of a single flaring loop can still be valid, but these flares may be subject to non-uniform heating across the loop (cf. Sylwester et al. 1990b).

4. Summary and conclusions

The aim of the present paper is to show how to use soft X-ray observations of solar flares in the analysis of their heating functions. Based on 32 flare models calculated by means of the Palermo–Harvard hydrodynamic code we have shown that the evolutionary paths in the emission measure–temperature diagrams are very sensitive to the variations of the heating function, $E_H(t)$. This in turn, allows us to use emission measure–temperature diagrams as diagnostic diagrams to study the time variations of the flare energy release, $E_H(t)$, of real solar flares.

We have applied our method to infer information about the heating functions of solar flares observed by the Bent Crystal Spectrometer on SMM. The emission measure–temperature diagrams have been constructed for 66 solar flares. Five generic groups can be distinguished with regard to the character of the evolution during the decay phase of the flares. We have presented $(\sqrt{\varepsilon}-T)$ diagrams for 10 flares and discussed the time variations of their heating functions throughout the observed evolution.

The main findings of the paper are the following:

(1) The $(\sqrt{\varepsilon}-T)$ diagrams constructed using high-quality X-ray observations constitute a helpful tool which allows us to investigate the time variations of the thermal energy release rate, $E_H(t)$, in flares.

(2) The $(\sqrt{\varepsilon}-T)$ diagrams for 56% of the analysed flares (the diagrams from groups I–III) resemble those obtained for simple hydrodynamic flare models. It suggests that the assumptions made in the Palermo–Harvard modelling seem to be appropriate for real conditions in many solar flares. (Here we have in mind the assumptions concerning uniform energy release across a loop of constant cross sectional area.)

(3) The flares whose emission measure–temperature diagrams belong to groups IV and V seem to be much more complicated. They probably involve a set of distinct loop structures within the same flaring region which dominate successively the soft X-ray emission during the flare evolution. It is also possible that such flares undergo non-uniform heating across the loop.

We have found that for an overwhelming majority of flares (more than 80% in our analysis) the heating operates well into the decay phase, with rates of heating decay of the order of minutes.

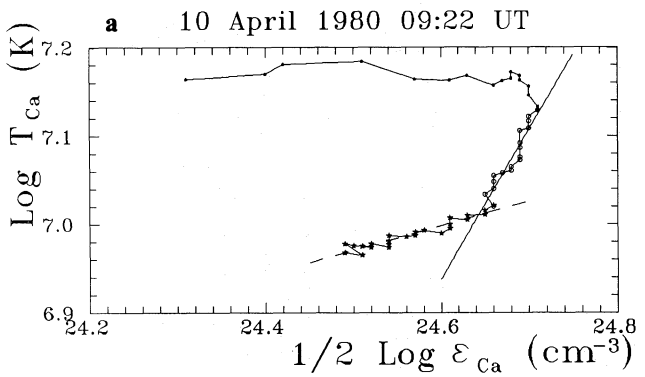

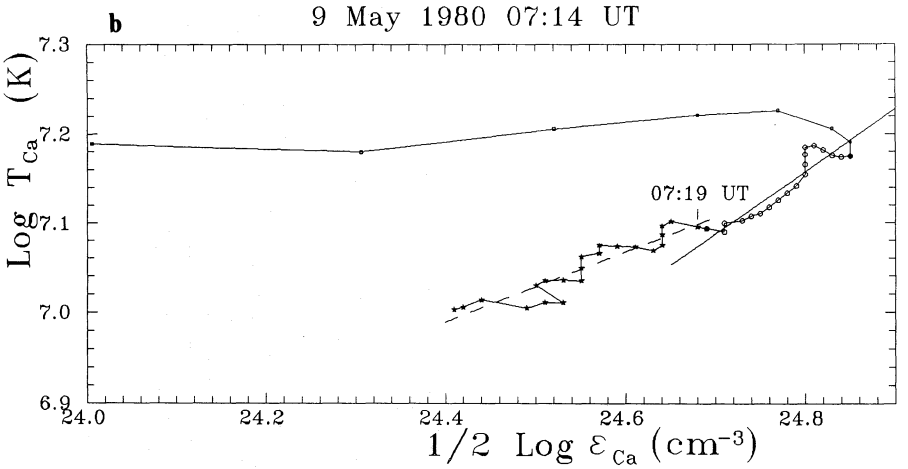

Fig. 8a and b. Same as Fig. 7 for flares: on 1980 April 10 at 09:22 UT (**a**) and on 1980 May 9 at 07:14 UT (**b**)

The above conclusions should be taken into account when developing models describing the process of energy release in flares.

Acknowledgements: We would like to thank Prof. J. Jakimiec for critically reading the manuscript and the referee, Prof. E.R. Priest who greatly helped to improve the text. This work has been supported by the Polish Academy of Sciences, by Agenzia Spaziale Italiana, the Italian National Research Council (CNR) and Ministero dell'Universita e della Ricerca Scientifica e Tecnologica and by Science Engineering Research Council.

References

Acton L.W., Culhane J.L., Gabriel A.H., et al., 1980, Sol. Phys. 65, 53

Chung-Chieh Cheng, Pallavicini R., 1984, Sol. Phys. 93, 337

Dennis B.R., Orwig L.E., Kiplinger A.L., et al., 1988. NASA Technical Memorandum 4036

Doschek G.A., Feldman U., Landecker P.B., McKenzie D.L., 1981, ApJ 249, 372

Duijveman A., Hoyng P., 1983, Sol. Phys. 86, 279

Duijveman A., Hoyng P., Machado M.E., 1982, Sol. Phys. 81, 137

Fludra A., Lemen J.R., Jakimiec J., Bentley R.D., Sylwester J., 1989, ApJ 344, 991

Jakimiec J., Sylwester B., Sylwester J., Lemen J.R., Mewe R., Bentley R.D., Peres G., Serio S., Schrijver J., 1986, Adv. Space Res. 6, 237

Jakimiec J., Sylwester B., Sylwester J., Lemen J.R., Mewe R., Bentley R.D., Peres G., Serio S., Schrijver J., 1987, in: Stepanov V.E., Obridko V.N. (eds.) Solar Maximum Analysis. VNU Science Press, Utrecht, p. 91

Jakimiec J., Sylwester B., Sylwester J., Serio S., Peres G., Reale F., 1992, A&A 253, 269 (Paper II)

Machado M.E., 1983, Sol. Phys. 89, 133

Machado M.E., Somov B.V., Rovira M.G., de Jager C., 1983, Sol. Phys. 85, 157

Peres G., Rosner R., Serio S., Vaiana G.S., ApJ 252, 791

Serio S., Reale F., Jakimiec J., Sylwester B., Sylwester J., 1991, A&A 241, 197 (Paper I)

Speich D.M., Nelson J.J., Licit J.P., Tolbert A.K., 1991, NASA Technical Memorandum 4287

Sylwester J., 1988, Adv. Space Res. 8, 55

Sylwester J., 1990, in: Dezsö L. (ed.) The Dynamic Sun. Publ. of Debrecen Heliophys. Obs. 7, Debrecen, p. 212

Sylwester B., Sylwester J., Jakimiec J., Fludra A., Bentley R.D., Schrijver J., 1986, Contributions of the Astronomical Observatory Skalnate Pleso 15, 145

Sylwester B., Sylwester J., Jakimiec J., Serio S., Reale F., 1990a, in: Uchida Y., Canfield R.C., Watanabe T., Hiei E. (eds.) Lecture Notes in Physics, 387, Springer, Berlin, p. 188

Sylwester B., Sylwester J., Bentley R.D., Fludra A., 1990b, Sol. Phys. 126, 177